`Building Tomorrow's Society

Bâtir la Société de Demain

Fredericton, Canada

June 13 – June 16, 2018/ *Juin 13 – Juin 16, 2018*

CORRELATION BETWEEN DIFFERENT FACTORS CONTROLLING SHRINKAGE BEHAVIOUR OF GEOPOLYMER MORTAR

Alhamdan, Ahmad[1,3] and Soliman, Ahmed[2]
[1]MASc. Student, Department of Building, Civil and Environmental Engineering Concordia University, Montreal, Quebec Canada.
[3] ahmad.alhamdan@mail.concordia.ca
[2]Assistant Professor, Department of Building, Civil and Environmental Engineering Concordia University, Montreal, Quebec Canada.

Abstract: Cement industry produces large amounts of carbon dioxide causing many environmental problems including global warming and air quality deterioration. As an alternative to cement, many studies have been conducted on alkali-activated materials (so-called geopolymers). Geopolymers showed similar or better mechanical and durability performance compared to that of cement-based materials. However, shrinkage behaviour of geopolymer materials is still one of the main problems that impede its in-situ applications. Hence, this study focuses on investigating the interrelationship between different factors that control shrinkage behaviour of geopolymer materials. These factors include supplementary cementitious material type, activator type and concentration, and curing temperatures. The setting time, workability, compressive strength, autogenous and drying shrinkage of alkali-activated mortars (AAMs) were evaluated. Results showed that the effect of activator type and concentration on the shrinkage behaviour differs according to the curing temperature. Moreover, the relationship between autogenous and drying shrinkage was significantly affected by the type of supplementary cementitious material used. Generally, the curing temperature is the most controlling factor for shrinkage behaviour of AAMs tested and also showed a strong influence on the effects of other factors.

1 INTRODUCTION

Global concrete production has grown widely over the recent decades in line with the population growth and the need for more infrastructures. The high demand for concrete in the construction industry increased ordinary Portland cement (OPC) production. The depletion of natural resources and the significant environmental pollution associated with carbon dioxide (CO_2) emissions generated during cement manufacturing process are of major concerns. Alkali-activated binder (AAB) represents a promising alternative to OPC in many constructional applications (Yang et al. 2013).

AABs rely on alumina-silicate precursors, found naturally occurring (eg. metakaolin) or formed as industrial by-products (eg. fly ash, slag), leading to a significant reduction in carbon emission. AAB production requires an alkaline medium (eg. sodium silicate Na_2SiO_3) and water to chemically activate the precursor forming the cementitious material (Khale and Chaudhary 2007). This process (so-called "geopolymerization") initiates with the dissolution of silicon and aluminum ions from the precursors into the alkaline medium. The dissolved ions react under sufficient alkalinity to produce silicate and aluminate compounds which are converted to a poly (alumina-silicate) structure with interconnected silicate oxide

(SiO_4) and aluminate oxide (AlO_4) tetrahedral. Thereafter, the hardening stage is achieved through the poly-condensation of those hydrolyzed species (Provis and Bernal 2014). This process requires cations like Na+, or K+ to reduce the charge variation which may be due to the coordination of aluminum in whole structure (Duxson et al. 2007).

Despite the various advantages of utilizing AABs in the construction industry, their widespread use has been hindered due to several challenges. One of the main challenges is shrinkage. Shrinkage mechanism of alkali-activated binders is still not clear. Shrinkage can significantly affect AAB performance by inducing cracks under restrained conditions.

2 EXPERIMENTAL PROGRAM

2.1 Materials

In the present study, FA class-F and GGBS were used as the precursor materials. The chemical compositions and physical properties of the FA and GGBS are listed in Table 1. Sodium hydroxide with a purity level of 98% and sodium silicate (SiO2 (30%), Na2O (20%), H2O (50%), specific gravity 1.38 g/mL) were used to prepare the alkali activators. The alkali activator was prepared as the following: Distilled water was used to dissolve the NaOH solid at 3M, 6M, and 12M, and left overnight to cool down to the room temperature while covered to prevent carbonation. Sodium silicate solution was then mixed with the NaOH solution to form the alkali activator solution (mass of sodium silicate solution/ NaOH solution = 2). ASTM standard river sand was used as the fine aggregate material. The oven-dry, saturated surface dry specific gravity, and absorption of the standard sand used were 2.54, 2.55, and 0.08 %, respectively.

2.2 Mix proportion and specimen preparation

The mix proportions of the alkali activated fly ash and slag mortars are shown in **Table 2**. Two precursor blends were utilized in this study Fly ash (FA) and Slag (GGBS). Six AAM mixtures were designed using a solution made of three different NaOH concentrations to cover a wide range of concentrations (3, 6, and 12M) each mixed with a constant sodium silicate concentration. The mass ratio of sand to precursor was fixed at 2:1 for all mixtures. The mass ratio of activator solution to precursor was 0.40 for all mixtures. The mass ratio of the water glass to NaOH solution was 2.0 in all activator mixtures. Two curing regimes were applied: 23°C with relative humidity of 60 ± 5% (ambient) and at 60°C (oven).

Table 1: Properties of precursors used.

Chemical composition (%)	Fly ash (FA)	Slag (GGBS)
CaO	2.60	56.10
SiO_2	46.00	21.00
Al_2O_3	33.00	17.00
Fe_2O_3	10.50	0.62
SO_3	-	0.77
Physical properties		
S.S.D Specific gravity (g/cm^3)	2.38	2.90
Surface area (m^2/kg)	290 (Blaine)	laine)

2.3 Specimen preparation

Initially, fly ash was dry mixed with sand in an electric mixer at a slow speed of (140 ± 5 revs/min) and medium speed (285 ± 5 revs/min) for 2 minutes to ensure homogeneity of the mixture. The prepared alkali activator solution is then added to the mixture and mixed for an additional 2 minutes. Immediately after mixing, 50 mm cubic molds for compressive strength evaluation according to ASTM Standard C109 / C109M-16a, and 25 mm × 25 mm × 285 mm prismatic molds for shrinkage measurements according to ASTM Standard C490 / C490M – 17, were cast. Specimens were compacted using a vibrating table and a tamping rod. All specimens were cured at room temperature of 23 °C and at a relative humidity of 60% ±

5% inside molds for 24 hours. After 24 hours, specimens were demolded and stored in ambient room conditions or in the oven at 60°C until testing age. All reported results represent the average of three replicates.

Table 2: Mix proportion of 1 m^3 alkali-activated mortar (AAM) specimens.

Mixture	FA (kg)	GGBS (kg)	NaOH solution molarity (M)	NaOH solution (kg)	Na_2SiO_3 solution (kg)	Sand (kg)
F3	655	0	3	87.33	174.67	1,310
F6	655	0	6	87.33	174.67	1,310
F12	655	0	12	87.33	174.67	1,310
S3	0	627	3	83.6	167.2	1,254
S6	0	627	6	83.6	167.2	1,254
S12	0	627	12	83.6	167.2	1,254

2.4 Testing program

The workability and flow of mortar mixtures were evaluated using the procedure listed in ASTM Standard C1437-15. Initial and final setting times were measured using a Vicat needle as described in ASTM Standard C191-13. Compressive strength development was evaluated at ages of 1, 7, 14, and 28 days using a 300 kN universal testing machine (UTM) in accordance with ASTM Standard C109 / C109M-16a. Cubes were loaded until failure at a load rate of 345 kPa/s. Cubic specimens (50 × 50 × 50 mm) were prepared for compressive strength measurements. The mortar cubes were compacted using a vibrating table and a tamping rod. Cubes were loaded until failure at a load rate of 345 kPa/s. Autogenous and drying shrinkage strains were measured using prism samples (25.4 × 25.4 × 254 mm) in accordance with ASTM Standard C490 / C490M - 17 using a length comparator with dial gauge accuracy of 0.0001-inch. After demolding, autogenous shrinkage specimens were wrapped with a first layer of polyethylene film and a second layer of aluminum foil to prevent any moisture loss.

3 EXPERIMENTAL RESULTS

3.1 Flowability

Variations in flowability for different alkali-activated mortar (AAM) mixtures with respect to NaOH concentrations are shown in **Table 3**. In general, the flow of AAMs decreased with the increase in the molar concentration of NaOH in the activating solution. For instance, reductions in the average flow of AAF mortars when NaOH concentrations increased from 3M to 6M and 12M were 5.56%, and 14.81%, respectively. Na_2SiO_3 liquid (waterglass) is known to have high viscosity itself hence, the mixture of waterglass with highly concentrated NaOH solutions tend to further increase the viscosity of the activating mixture and thus reduce the flow of AAM (Chindaprasirt et al. 2007). Moreover, the flowability of AAS mortars was lower than that of the AAF mortars at similar NaOH concentration.

3.2 Setting time

Setting time tests were performed in order to ascertain the effects of precursor type and NaOH solution molarity on the stiffing of AAM. Initial and final setting time results of different AAM are shown in **Table 3**. Generally, higher NaOH concentrations accelerated both the initial and final setting behavior of AAM mixtures. For instance, reductions in the initial setting time of AAF mortars when NaOH concentrations increased from 3M to 6M and 12M were 12.5%, and 38.2%, respectively. The corresponding reductions in final setting times were 11.2% and 35%, respectively. Higher activator concentrations tend to accelerate the rate of the hydration reaction hence, directly influencing the stiffness behavior of AAMs. AAS mortar mixtures exhibited faster settings compared to AAF mortar mixtures. For example, the initial setting in 3M NaOH activated slag mortars was achieved 36 minutes earlier than in 3M NaOH activated fly ash.

Table 3: Setting time and flow values of AAM mixtures.

Mixture	Setting time (min)		Flowability (cm)
	Initial	Final	
F3	144	286	108
F6	126	254	102
F12	89	186	92
S3	108	171	94
S6	72	114	87
S12	47	76	76

3.3 Compressive strength

3.3.1 Effect of activator concentrations

The compressive strength development of AAM mixtures activated with different concentrations of NaOH was studied**. Figure 1** shows the compressive strength of AAF mortars. Generally, the compressive strength of AAF mortars increased with higher activator concentrations under both curing conditions. For instance, when NaOH concentration increased from 3M to 6M and 12M, the 28 days compressive strength of ambiently cured AAF mortars increased by 46.2%, and 117.26%, respectively. The increase in 28 days compressive strength of oven cured AAF mortars due to higher NaOH concentrations was almost equal to the one found in ambient cured ones. **Figure 2** shows the compressive strength of AAS mortars. Similar compressive strength increase trend with higher NaOH concentrations was found in AAS mortars.

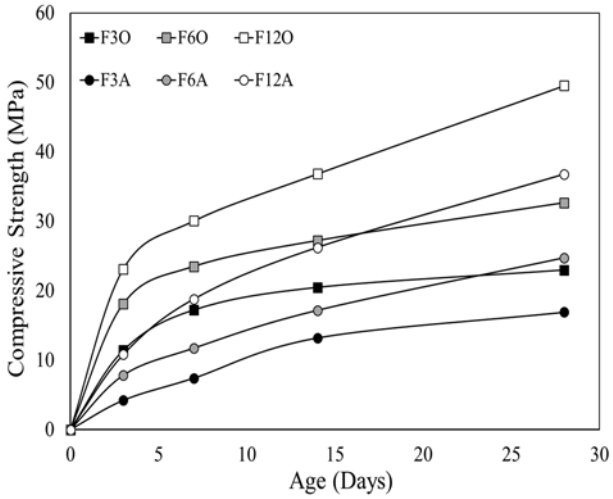

Figure 1: Compressive Strength of AAF mortar specimens (ambient (A) and oven (O) cured).

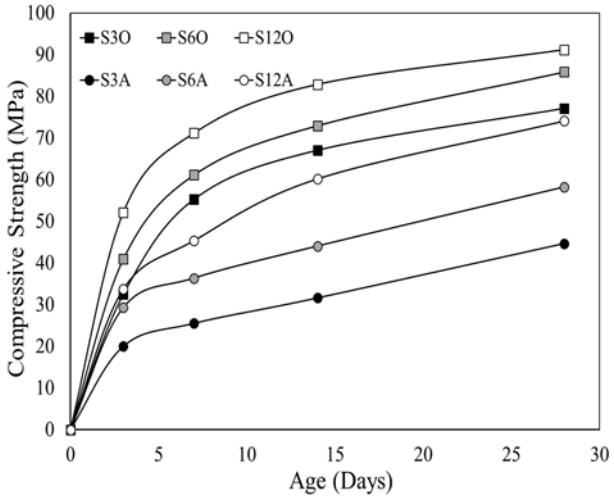

Figure 2: Compressive Strength of AAS mortar specimens (ambient (A) and oven (O) cured).

3.3.2 Effect of precursor type

Compressive strength results for all mortar specimens activated with 3M, 6M, and 12M (NaOH) concentrations and cured at both conditions are plotted in **Figs. 1 and 2**. Generally, AAM specimens exhibited steady strength development between 3 and 28 days. AAS mortar specimens achieved higher 28 days compressive strength than AAF mortars under both curing conditions. For instance, at low activator molarities (3M NaOH), the 28 days compressive strength of ambient cured AAS mortars was 160% higher than that of AAF mortars. The corresponding compressive strength of oven cured AAS mortars was 263% higher than that of AAF mortars.

3.3.3 Effect of curing temperature

Compressive strength results of AAF and AAS mortars activated with different NaOH concentration and cured at ambient and oven conditions are shown **Figs. 1 and 2**. Results indicated that all specimens cured in the oven had acquired extra compressive strength during the 28 days study period. For instance, the 28 days compressive strength values of ambient cured AAF mortars activated with 3M, 6M, and 12M NaOH concentrations were increased by 36, 32, and 35%, respectively when cured in the oven. Normally, the activation reaction of fly ash at room temperature is slow (Shi and Day 1999). On the other hand, previous research showed that GGBS can be activated effectively at room temperature by an alkaline medium (Shi and Day 1999). As expected, ambient cured AAS mortars activated with 3M, 6M, and 12M NaOH concentrations achieved high 28 days compressive strength results of 44.67, 58.22, and 74.11 Mpa, respectively.

3.4 Drying Shrinkage

3.4.1 Effect of activator concentrations

Shrinkage is a critical parameter for long-term serviceability of concrete structures. The drying shrinkage strains for AAM activated with different (NaOH) concentrations and cured at ambient and oven temperatures are plotted in **Figs. 3 and 4**. Typically, the magnitude and rate of drying shrinkage in all AAM specimens increased with higher NaOH concentrations. Around 80-86 % of the total shrinkage was observed within the first 7 days depending on activator concentrations. For instance, the drying shrinkage strain experienced by 12M NaOH activated AAF mortars was 25%, and 34% more than the ones experienced by 6M, and 3M NaOH activated mortars, respectively under ambient curing. The corresponding drying shrinkage strains under oven curing were also 18%, and 27% higher, respectively.

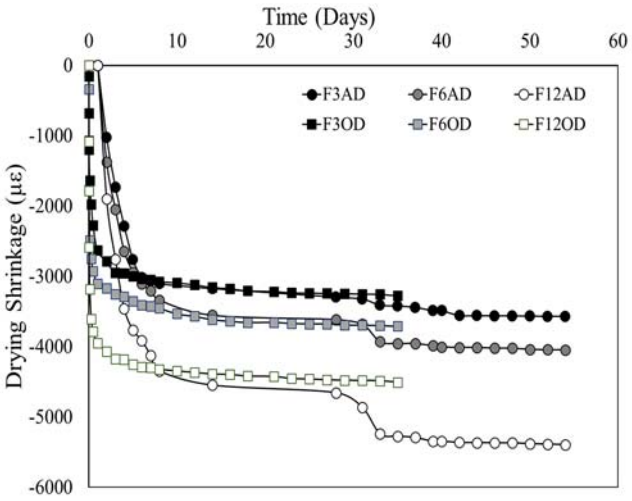

Figure 3: Drying shrinkage of AAF mortar specimens (ambient and oven cured).

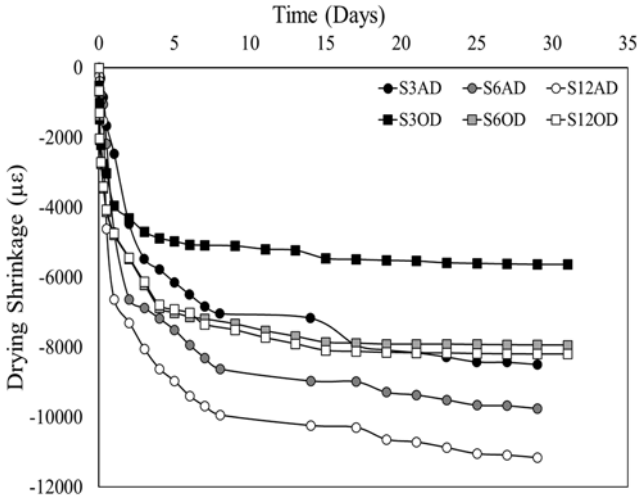

Figure 4: Drying shrinkage of AAS mortar specimens (ambient and oven cured).

3.4.2 Effect of precursor type

The effect of precursor type on drying shrinkage of AAMs was evaluated. Drying shrinkage strains of different mortar specimens activated with 3M, 6M, and 12M (NaOH) concentrations and cured at ambient temperature are plotted in **Figs. 3 and 4**, respectively. Results indicated that AAS mortars experienced higher drying shrinkage strains compared to AAF mortars. For instance, at low activator concentration (3M NaOH), the drying shrinkage strains of AAS mortars ambient and oven cured were 71.8%, and 142% higher than those measured in AAF mortars, respectively. Around 81-85 % of the total drying shrinkage was observed in the first 7 days. These results are in agreement with the literature (Fernández-Jimenez et al. 2006, Chi and Huang 2013).

AAS binders are known to have a high percentage of mesopores compared to AAF and OPC binders (Chen and Brouwers 2007). Consequently, the more refined pores found in AAS resulted in higher capillary stress which in turns significantly increased the drying shrinkage. Moreover, the spherical shape of fly ash particles tends to act as micro-aggregate and fills minor voids hence, increasing the volume stability of AAF mortars (Rashad 2013).

3.4.3 Effect of curing temperature

One of the major obstacles challenging the implementation of AABs in the industry is the requirement for a high curing temperature to obtain the expected superior properties over ordinary PC products. The effect of curing condition on different AAMs at several activator concentrations was studied. Drying shrinkage strains of AAF and AAS mortars cured at both ambient and oven conditions are shown in **Figs. 3 and 4**, respectively. Generally, the drying shrinkage strains were reduced in all mortar specimens cured in the oven at 60 °C compared to the ones cured at ambiance. The value of shrinkage reduction had a correlation with both precursor type and activator concentration. In AAF mortars, the shrinkage of oven cured mortars activated with 3M, 6M, and 12M NaOH concentrations were decreased by around 8.16, 8.31, and 16.41%, respectively compared to ambient cured specimens.

3.5 Autogenous Shrinkage

3.5.1 Effect of activator concentration

Autogenous shrinkage is caused by self-desiccation which is a result of the formation of finer pores in the microstructure of hardened binder and the water consumption by the continued hydration reaction (Lee et al. 2014). The autogenous shrinkage strains of AAF and AAS mortars activated with different (NaOH) concentrations and cured at ambient and oven temperatures are plotted in **Figs. 5 and 6**, respectively.

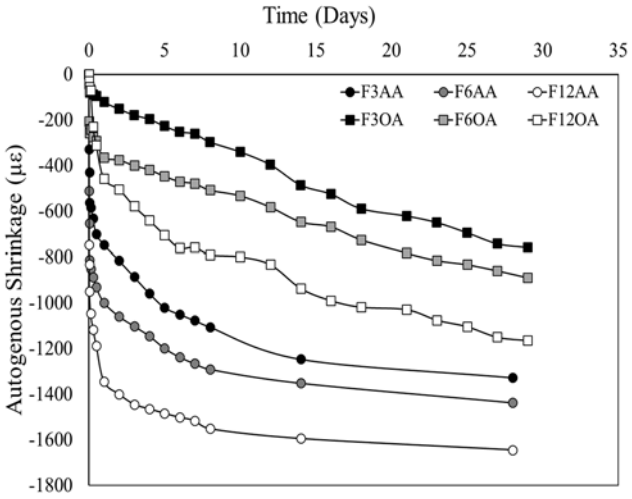

Figure 5: Autogenous shrinkage of AAF mortars (ambient and oven cured).

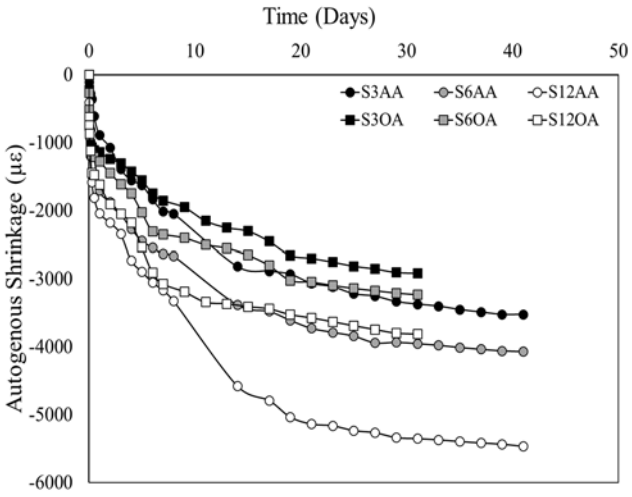

Figure 6: Autogenous shrinkage of AAS mortars (ambient and oven cured).

Generally, autogenous shrinkage rates and strains of AAMs increased with higher activator concentrations. For instance, the autogenous shrinkage strain experienced by 12M NaOH activated fly ash mortars was 9.3%, and 19.3% more than the ones experienced by 6M, and 3M NaOH activated mortars, respectively under ambient curing. The corresponding autogenous shrinkage strains under oven curing were also 28.5%, and 55.7% higher, respectively.

3.5.2 Effect of precursor type

Autogenous shrinkage strains for different mortar specimens activated with 3M, 6M, and 12M (NaOH) concentrations and cured at ambient temperature are plotted in **Figs. 5 and 6**. Generally, AAS mortars experienced the higher autogenous shrinkage strains compared to AAF mortars. For example, the autogenous shrinkage strain of ambient cured AAS mortar was 144% higher than that of AAF mortars when activated with low activator concentrations (3M NaOH). The corresponding autogenous shrinkage strain under oven curing was also 71.8% higher. For AAMs activated with high activator concentrations (12M), the drying shrinkage strain of AAS mortar was 217% higher than the one experienced by AAF mortars under ambient curing. The corresponding drying shrinkage under oven curing was 63%, and 275% higher, respectively. These results give an idea of the much better dimensional stability of AAF mortar compared to AAS mortars.

3.5.3 Effect of curing condition

Autogenous shrinkage results of AAF and AAS mortars cured at both ambient and oven conditions are shown in **Figs. 5 and 6**, respectively. Generally, the autogenous shrinkage strains were reduced in all AAM specimens cured in the oven at 60 °C compared to the ones cured at ambiance. Reduction in autogenous shrinkage strains due to oven curing was slightly more pronounced in AAF mortars and almost equal to AAS mortars. For instance, the autogenous shrinkage strains experienced by 3M, 6M, and 12M NaOH activated AAF mortars were reduced by around 46.4, 40.5, and 30%, respectively when oven curing is adopted. The corresponding reductions in AAS mortars were 17.24, 20.58, and 30%, respectively.

4 CONCLUSION

- Setting time and flowability of AAMs seem to be affected directly by the activator concentrations, as concentrations increase, both formers decrease.
- The strength of the AAMs depends highly on the activator dosage, as it was clear that higher NaOH dosages increased the compressive strength at all ages regardless of precursor type used.
- The autogenous and drying shrinkage strains experienced by AAMs were significantly higher than the ones found in OPC mortar.

- Regardless of the activator concentrations, AAS mortars exhibited higher drying and autogenous shrinkage strains compared to AAF mortars.

References

ASTM C109 / C109M-16a, Standard Test Method for Compressive Strength of Hydraulic Cement Mortars (Using 2-in. or [50-mm] Cube Specimens), ASTM International, West Conshohocken, PA, 2016, www.astm.org

ASTM C1437-15, Standard Test Method for Flow of Hydraulic Cement Mortar, ASTM International, West Conshohocken, PA, 2015, www.astm.org

ASTM C191-13, Standard Test Methods for Time of Setting of Hydraulic Cement by Vicat Needle, ASTM International, West Conshohocken, PA, 2013, www.astm.org

ASTM C490 / C490M-17, Standard Practice for Use of Apparatus for the Determination of Length Change of Hardened Cement Paste, Mortar, and Concrete, ASTM International, West Conshohocken, PA, 2017, www.astm.org

Chen, W., and Brouwers, H. J. H. 2007. The Hydration of Slag, Part 1: Reaction Models for Alkali-Activated Slag. *Journal of Materials Science*, **42**(2): 428-443.

Chi, M., and Huang, R. 2013. Binding Mechanism and Properties of Alkali-Activated Fly Ash/Slag Mortars. *Construction and Building Materials*, **40**: 291-298.

Chindaprasirt, P., Chareerat, T., and Sirivivatnanon, V. 2007. Workability and Strength of Coarse High Calcium Fly Ash Geopolymer. *Cement and Concrete Composites*, **29**(3): 224-229.

Duxson, P., Provis, J. L., Lukey, G. C., and Van Deventer, J. S. 2007. The Role of Inorganic Polymer Technology in the Development of 'Green Concrete'. *Cement and Concrete Research*, **37**(12): 1590-1597.

Fernández-Jimenez, A. M., Palomo, A., and Lopez-Hombrados, C. 2006. Engineering Properties of Alkali-Activated Fly Ash Concrete. *ACI Materials Journal*, **103**(2), 106.

Khale, D., and Chaudhary, R. 2007. Mechanism of Geopolymerization and Factors Influencing its Development: A Review. *Journal of Materials Science*, **42**(3): 729-746.

Lee, N. K., Jang, J. G., and Lee, H. K. 2014. Shrinkage Characteristics of Alkali-Activated Fly Ash/Slag Paste and Mortar at Early Ages. *Cement and Concrete Composites*, **53**: 239-248.

Ma, Y., Hu, J., and Ye, G. 2013. The Pore Structure And Permeability Of Alkali Activated Fly Ash. *Fuel*, **104**: 771-780.

Provis, J. L., and Bernal, S. A. 2014. Geopolymers and Related Alkali-Activated Materials. *Annual Review of Materials Research*, **44**: 299-327.

Rashad, A. M. 2013. Properties Of Alkali-Activated Fly Ash Concrete Blended With Slag. *Iran J Mater Sci Eng*, **10**(1): 57-64.

Shi, C., and Day, R. L. 1999. Early Strength Development and Hydration of Alkali-Activated Blast Furnace Slag/Fly Ash Blends. *Advances in Cement Research*, **11**(4): 189-196.

Yang, K. H., Song, J. K., and Song, K. I. 2013. Assessment of CO2 Reduction of Alkali-Activated Concrete. *Journal of Cleaner Production*, **39**: 265-272.